Author/s:
Xu, Y;Zhou, J;Smith, TA

Title:
Time-resolved emission microscopy of light-induced aggregation of luminescent polymers

Date:
2019-12-23

Citation:
Xu, Y., Zhou, J. & Smith, T. A. (2019). Time-resolved emission microscopy of light-induced aggregation of luminescent polymers. Methods and Applications in Fluorescence, 8 (1), https://doi.org/10.1088/2050-6120/ab5976.

Persistent Link:
https://hdl.handle.net/11343/345202

Methods and Applications in Fluorescence

Time-resolved emission microscopy of light-induced aggregation of luminescent polymers

To cite this article before publication: Yang Xu *et al* 2019 *Methods Appl. Fluoresc.* in press https://doi.org/10.1088/2050-6120/ab5976

Time-Resolved Emission Microscopy of Light-Induced Aggregation of Luminescent Polymers

Yang Xu,[†] Jian Zhou[‡] and Trevor A. Smith[†*]

[†]ARC Centre of Excellence in Exciton Science, School of Chemistry, University of Melbourne, 3010 Victoria, Australia
[‡]College of Material, Chemistry and Chemical Engineering, Hangzhou Normal University, Hangzhou 310036, China

E-mail: trevoras@unimelb.edu.au

6 November 2019

Abstract.

Photon pressure has been used induce the aggregation from solution of a series of photoluminescence conjugated polyelectrolytes containing tetraphenylethene units. These polymers show steady-state and time-resolved emission properties that are dependent on the local chromophore environment that can be influenced by the degree of intra- and inter-molecular interactions, which enables the photoaggregation process to be monitored by time-resolved fluorescence imaging techniques. Structural differences in the polymer lead to variations in the photo-induced aggregation behaviour.

1. Introduction:

1.1. Photon Pressure and Optical Trapping

The momentum carried by photons can be transferred from the propagating light beam to matter through the combination of forces induced when light is refracted as it passes from a medium of one refractive index to a second medium of a different refractive index. The net force that is applied to the second medium can be exploited to induce various influences on that medium. One of these effects is the optical force, or pressure, exerted by light incident upon particles smaller than the wavelength of the light. The photon pressure exerted on such a Rayleigh particle can expressed as:

$$F = \frac{1}{2}\alpha\nabla\mathbf{E}^2 + \alpha\frac{\delta}{\delta t}(\mathbf{E}\times\mathbf{B}) \quad or \quad \frac{1}{2}\alpha\nabla\mathbf{E}^2 + \frac{n_m\langle\mathbf{E}\times\mathbf{B}\rangle C_{scat}}{c} \tag{1}$$

where $\mathbf{E}$ and $\mathbf{B}$ are the electric field strength and magnetic flux density, respectively, and ∇ represents a gradient with respect to the spatial coordinates. α is the polarizability of the

particle under the dipole approximation, and when the particle is modelled in a dielectric medium, α is given by:

$$\alpha = 4\pi\epsilon_m r^3 \frac{\left(\frac{n_p}{n_m}\right)^2 - 1}{\left(\frac{n_p}{n_m}\right)^2 + 2} \tag{2}$$

where r is the radius of the particle, n_p and n_m are the refractive indices of the particle and the surrounding medium, respectively, and ϵ_m is the permittivity of the surrounding medium. C_{scat} and c represent the light scattering cross section of the nanoparticle, and the speed of light in a vacuum, respectively.

The transfer of momentum and the resulting forces can be used to optically trap particles of a refractive index different to that of their surrounding medium.[1, 2] This work culminated in the 50% award of the 2018 Nobel Prize for Physics to Ashkin. The photon pressure effect can be used for applications beyond simply laser trapping large (Mie-sized) particles.[3] The angular momentum that can be imparted from light to birefringent materials has also led to light-driven rotation in "micromachines".[4] Photon pressure has been used to investigate and control the behaviour of polymers. Of particular relevance here is the photo-induced assembly of polymers and other materials from solution, and light-induced crystallisation; research areas principally led by Masuhara and co-workers. Ishikawa[5] used photon pressure to produce reversible microparticles of poly(N-isopropylacrylamide) through local heating of water by a laser and the phase transition of the polymer solution. Conjugation of polystyrene in individual micron-diameter particles has been investigated in which double-bond formation in the backbone of the polymer chain that can lead to polymer degradation, was monitored by observing the magnitude and duration of emission from the polymeric particles.[6] Shpaisman et al.[7] used optical traps to influence an ongoing polymerization process of emulsion droplets. Ito et al. [8] demonstrated localised photopolymerisation of microstructures smaller than diffraction limit of the trapping light by inducing one-photon UV polymerisation of liquid acrylate solutions in the optical-trapping potential of a focused near-IR (NIR) laser beam.

1.2. Time-Resolved Emission Imaging

In most of the above cited works on photon pressure-induced phenomena, steady state emission techniques and backscattered laser radiation were primarily used to characterise the optical effects induced by photon pressure, but to date, reports using time-resolved emission spectroscopic techniques have been very limited. Borowicz et al.[9] used photon pressure to study microparticle formation of poly(N-vinylcarbazole) in N,N-Dimethylformamide solution by both steady-state and time-resolved fluorescence measurements. In previous work[10] two kinds of water-soluble carbazolyl-containing copolymers in aqueous solution were shown to result in the formation of single microparticles. The two different polymers were shown to photo-aggregate at different rates. The rate of particle formation and the final particle size were found to be shorter and larger, respectively, as the carbazolyl content of the polymer was higher. This indicated that the polarisability of the polymer plays an important role in the photon pressure-induced association process. That work was hampered by the polymers studied only being emissive in the ultraviolet region (requiring a UV microscope

to perform any time-resolved measurements simultaneous with photon aggregation) and spectral and temporal changes due to any excimer formation between the carbazolyl groups were essentially undetectable.

1.3. Aggregation Enhanced Emission

It is well known that the emission of fluorophores is often strongly influenced by their local molecular environment. One manifestation of this is when the efficiency of vibrational and rotational relaxation is decreased (with a reduction in the non-radiative rate constant, k_{nr}), for example through molecular adsorption or increased viscosity, resulting in enhanced emission intensity (and concomitantly extended fluorescence decay times). Molecular aggregation can also lead to changes in the emission intensity (and fluorescence decay timescales); reduced emission (sometimes termed "concentration- or aggregation-caused quenching") can result from processes including electronic coupling and non-emissive aggregate formation, and the reduced molecular vibrational and/or rotational freedom due to the steric crowding in the aggregated state can lead to the enhancement of emission.

In this paper we report the use of photon pressure to aggregate a series of new conjugated polyelectrolytes (CPEs) containing tetraphenylethene (TPE) units.[11, 12] These polymers are photoluminescent from cyan to red and exhibit enhanced emission properties due to aggregation, with small spectral shifts and a marked increase in fluorescence quantum yield (and hence longer fluorescence decay times), upon changes in solvent quality. These changes are attributed to the reduction in the rate of the non-radiative deactivation pathways due to restriction of the rotational motion of the groups within the TPE core in the excited state, as the polymer adopts a more coiled structure to avoid interaction with the poorer solvent. In the better solvent the molecular configuration will be more open to optimise these interactions.

Upon photon-induced aggregation, similar restrictions on the non-radiative pathways might be expected, but will not be readily identifiable through spectral changes. On the other hand, the photo-aggregation should be readily detected through changes in emission decay behaviour. In this work we have coupled photon-pressure induced aggregation with time-resolved emission microscopy techniques. We have monitored the extent of photo-aggregation by time-resolved fluorescence measurements as a function of irradiation time. We show significant changes in the fluorescence decay profiles of the polymer as it aggregates, and that this aggregation is dependent on the polymer structure.

2. Experimental Methods

2.1. Sample Preparation

A series of conjugated polyelectrolytes (CPEs) containing tetraphenylethene units have been synthesised and characterised, as reported elsewhere.[11] The molecular structures of the polyelectrolytes; $P1^+$, $P2^+$ and $P3^+$, are given in Figure 1. Solutions of each polymer were prepared in dimethyl sulfoxide (DMSO) to concentrations of 100 μM. A droplet of the solution was placed in a cavity microscope slide (Sailing Boat, cat# 7103), covered with a

coverslip and sealed with Super Glue.

Dynamic light scattering measurements were performed on solutions of the same concentrations as were used for the photoaggregation experiments, using a Brookhaven system (BI-200SM) based on a HeNe laser at 633nm, and operated in both multi-angle and 90° modes.

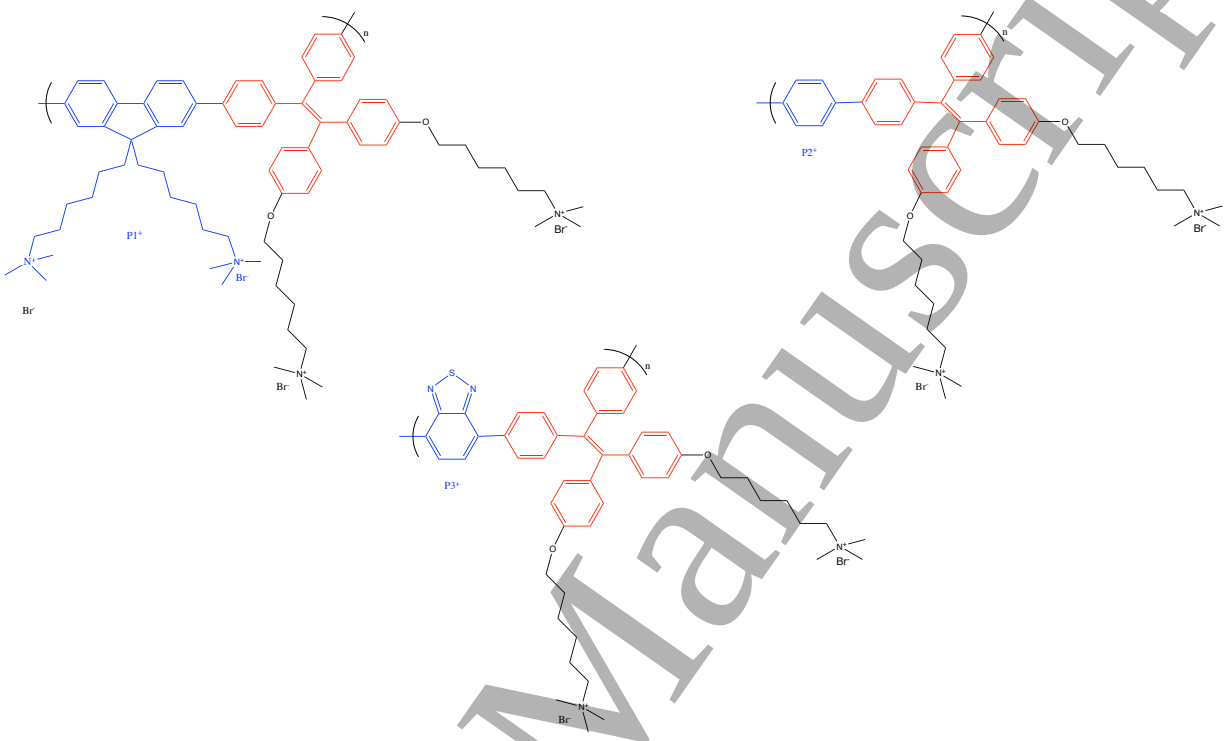

Figure 1: Molecular structures of $P1^+$, $P2^+$ and $P3^+$.

2.2. Photon Pressure and Time-Resolved Imaging Apparatus

A schematic diagram of the apparatus is shown in Figure 2. The photon pressure beam was provided by a continuous wave Nd:YAG laser operating at 1,064 nm (Suwtech, DPIR-2500, maximum output = 530 mW, TEM_{00}). The beam was expanded using a pair of lenses (f_1=13.86mm and f_2=50.0mm), spatially filtered through a 25 μm pinhole and introduced through the modified fluorescence lamp port on the rear of an inverted microscope (Olympus, IX71). The IR beam was reflected vertically using a low-pass dichroic beamsplitter (Omega Optical 750DCSPXR) and filled the back aperture of a microscope objective (Olympus, UPlan SApo 100x Oil, 1.4 NA), used to focus the light through a coverslip into the solution of the relevant polymer contained in a concave microscope slide (Figure 3). The maximum power of the IR laser measured at the focal point of the microscope objective was ~20 mW.

The time-resolved emission imaging system comprised a modified Olympus FV300 confocal fluorescence scanner unit coupled to the same inverted microscope. The excitation source was the frequency doubled (400 nm) output of a mode-locked and cavity dumped Titanium:sapphire laser (Coherent Mira F/APE PulseSwitch). The pulse repetition rate was adjusted to 5.4 MHz. This beam was delivered by a single mode optical fibre (ThorLabs,

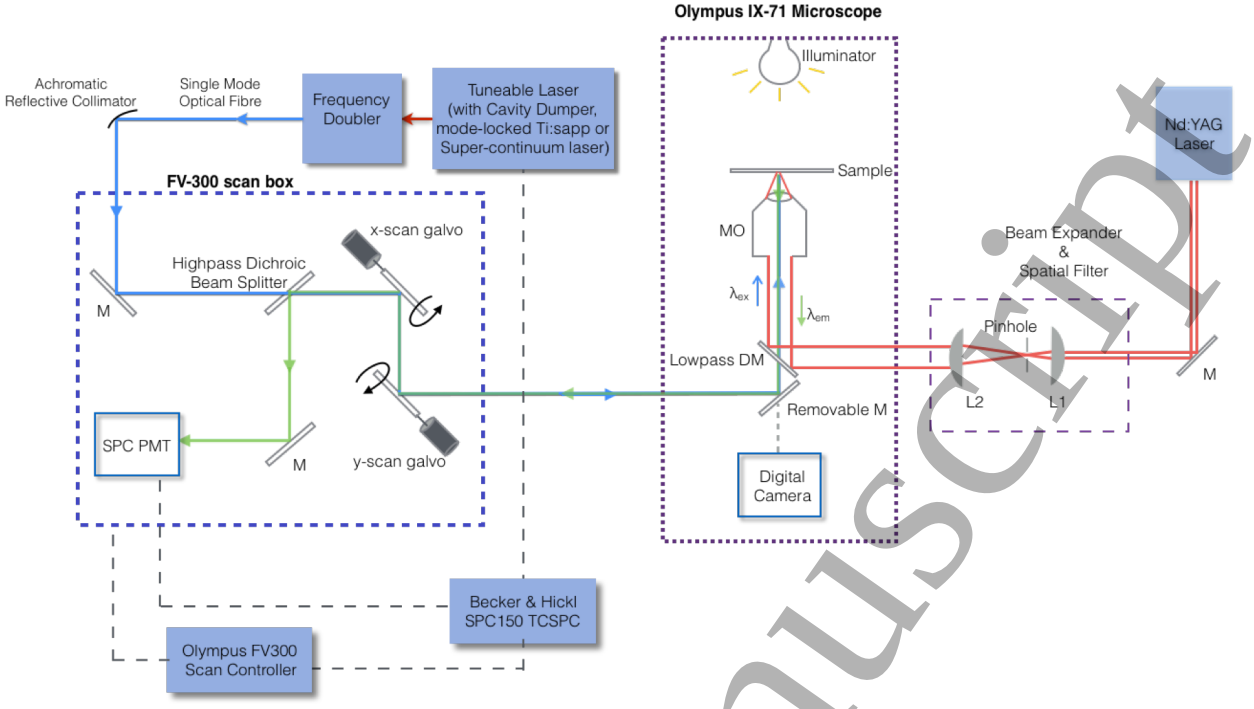

Figure 2: Schematic diagram of the photon pressure and time-resolved fluorescence imaging apparatus (DM represents dichroic mirrors, MO is the microscope objective lens).

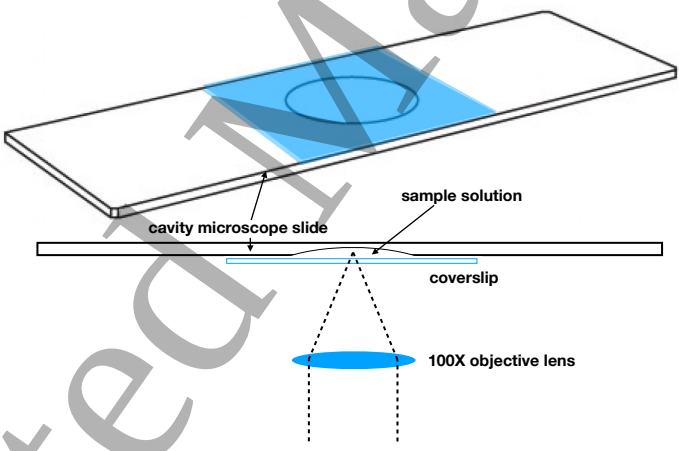

Figure 3: Sample in cavity microscope slide.

S305) to the scan head and collimated with an achromatic reflective collimator (ThorLabs, RC02SMA-F01). The beam from the galvanometer-based scan head was overlapped and centred with the IR beam at the short-pass dichroic beamsplitter and focussed with the same objective lens. The emission induced by the 400nm beam was collected with the same objective lens and passed through the same dichroic filter. The confocally isolated emission was detected, following a 520 nm highpass filter, via a modified output port on the scan head, by a single photon counting photomultiplier tube (Becker & Hickl, PMC100). A commercial time-correlated single photon counting system (Becker & Hickl SPC150 card, acquisition software (SPCM 9.78) and SPCImage software (version 7.0)) were used for the acquisition and analysis of the time-resolved emission data. The image acquisition was synchronised to

the frame, line and pixel clocks from the scanner. Samples were irradiated with the IR beam at a fixed fluence for periods of up to two hours. Simultaneously, time-resolved fluorescence images were recorded covering regions of the sample that included both the bulk solution as well as the photon-aggregated region; each image was acquired over 10 minutes at 5 or 10 minute intervals.

3. Results and Discussion

The polymers used in this study possess good solubility in DMSO and display weak emission in dilute DMSO solution,[11] however, when a large amount of THF, a poor solvent for the CPEs, is added to the DMSO solution strong emission is observed. The dramatic increase in emission intensity as the quality of the solvent is decreased is accompanied by a minor blue shift, but otherwise very little spectral change is observed.[11] This behaviour is attributed to the reduced freedom of movement within the molecule due to increased aggregation of the molecules in the poorer solvent.

Irradiation of each polymer sample in solution with the focused IR beam did not generate any emission from any of the samples, however, over a timescale of several tens of minutes of constant irradiation with the focussed IR beam the emission intensity gradually increased at the focal point compared to the bulk solution as observed through conventional confocal fluorescence and transmission images (not shown). The enhanced emission intensity is indicative of a increased local concentration of the CPEs at the focal point induced by the influence of photon pressure. However, steady-state (intensity-only) emission maps do not inform whether or not the emission increase is associated with other processes such as molecular aggregation. Time-resolved emission imaging, on the other hand, can clearly differentiate between simple concentration changes and the effects of other photophysical processes.

Time-resolved fluorescence images were generated by scanning the 400 nm mode-locked laser beam over regions of some tens of microns encompassing the bulk solution and the focussed IR beam, coupled with confocal fluorescence detection using the TCSPC technique. The increase in intensity at the focal point of the IR beam is associated with small increases in the temporal scales of the fluorescence decay behaviour of the polymer. The TCSPC-generated time-resolved fluorescence images were analysed based on a triple exponential decay function. Representative time-resolved fluorescence images mapping the amplitude average lifetime, τ_m, (Equation 3)[13] for each polymer as a function of irradiation time are shown in Figure 4. In each case, the τ_m images at early irradiation times simply show the fluorescence decay properties of the polymer in solution.

$$\tau_m = \frac{\sum_{i=1}^{N} a_i \tau_i}{\sum_{i=1}^{N} a_i} \tag{3}$$

Whilst the light-induced aggregated region does not appear significantly different in the τ_m maps (Figure 4(a, c, e)), the corresponding maps of the τ_3 component for each

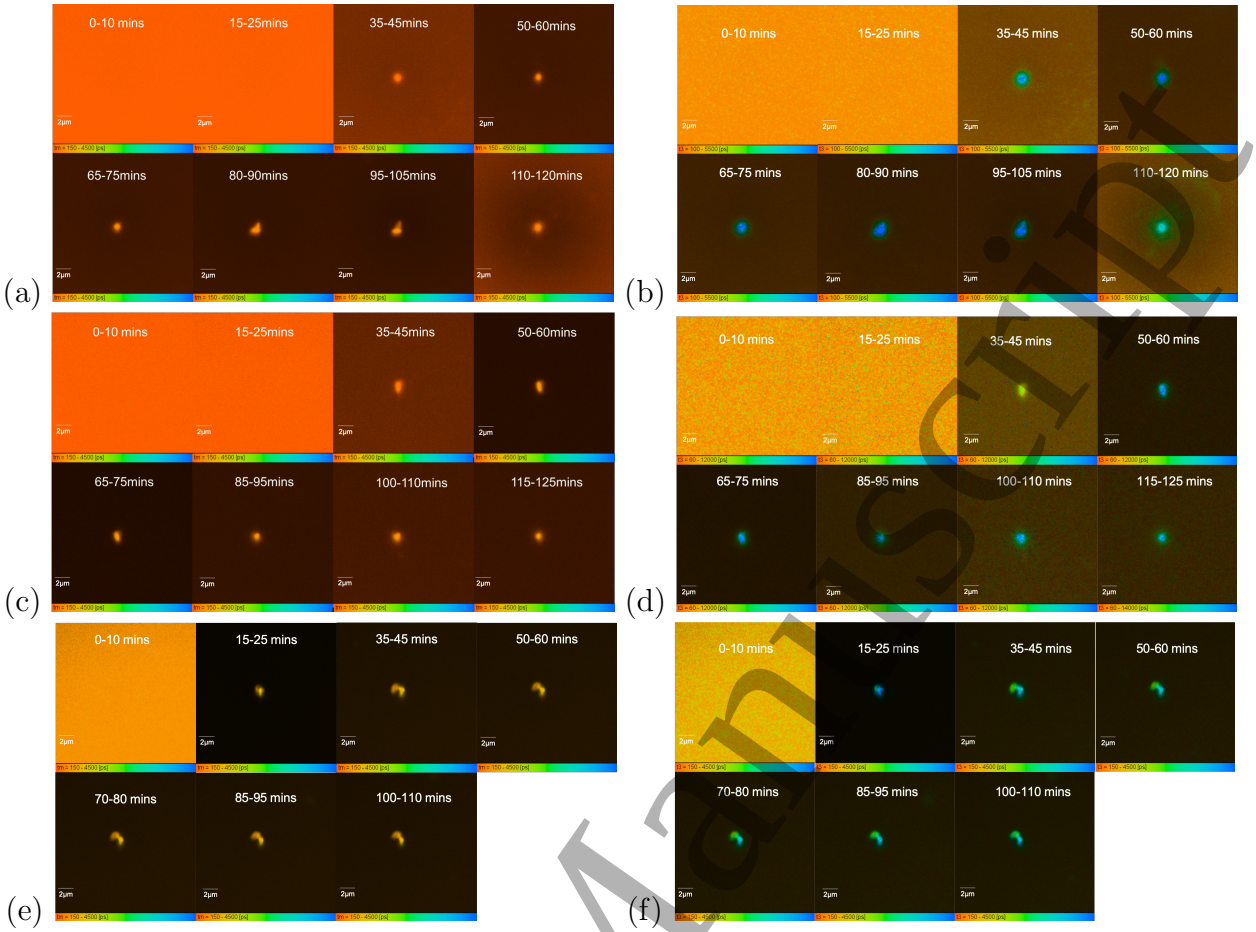

Figure 4: Time-resolved fluorescence images mapped as average lifetime, τ_m (a, c, e) and τ_3 component (b, d, f) of $P1^+$, $P2^+$ and $P3^+$, respectively, as a function of irradiation time.

polymer, shown in Figure 4(b, d, f), illustrate that the emission comprises a significant contribution from a longer-lived component. This is attributed to the photon pressure-induced aggregation of the polymer inhibiting rotational motion of the bonds within the TPE groups and thus providing increased competitiveness of the radiative deactivation pathway over the non-radiative pathways. This behaviour is masked/hidden through use of the average lifetime due to the small pre-exponential factor of the long lifetime component.

Representative fluorescence decay profiles from $P2^+$ in DMSO generated from a given region of pixels corresponding to the aggregated areas in the images recorded as a function of irradiation time are shown in (Figure 5). The increase in fluorescence intensity is clearly related to the increase in the integrated emission of the fluorescence decay profiles as the aggregated particles form. The decays reach a maximum in their emission timescale and then become a little shortened at long irradiation times. This is attributed to self/concentration quenching as the particle reaches a given size/density. Similar behaviour was observed for all three polymer solutions.

Close inspection of the time-resolved emission images (Figure 4) shows that the polymer $P3^+$ aggregated differently to the other two polymers. Rather than producing reasonably spherical particles, the $P3^+$ photon-aggregated region is asymmetrical, forming two "lobes".

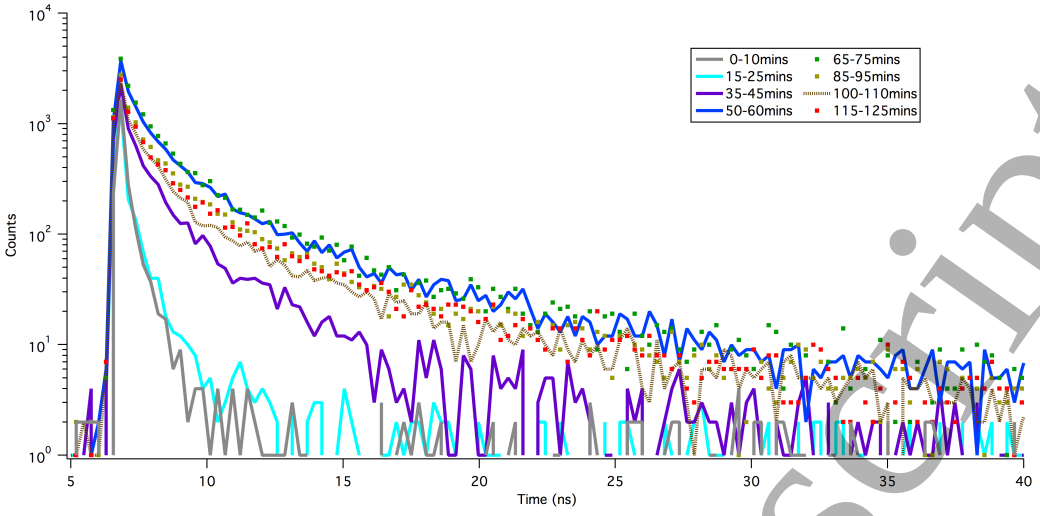

Figure 5: Fluorescence decay profiles of $P2^+$ in DMSO as a function of time.

This is somewhat reminiscent of the behaviour reported for 50-nm-sized polystyrene beads[14] or silica nanoparticles with different hydrophobic surface properties[15], in studies that were restricted to steady-state imaging methods. The time-resolved emission measurements of the $P3^+$ CPE show that these two "lobes" exhibit different fluorescence decay characteristics (Figure 6).

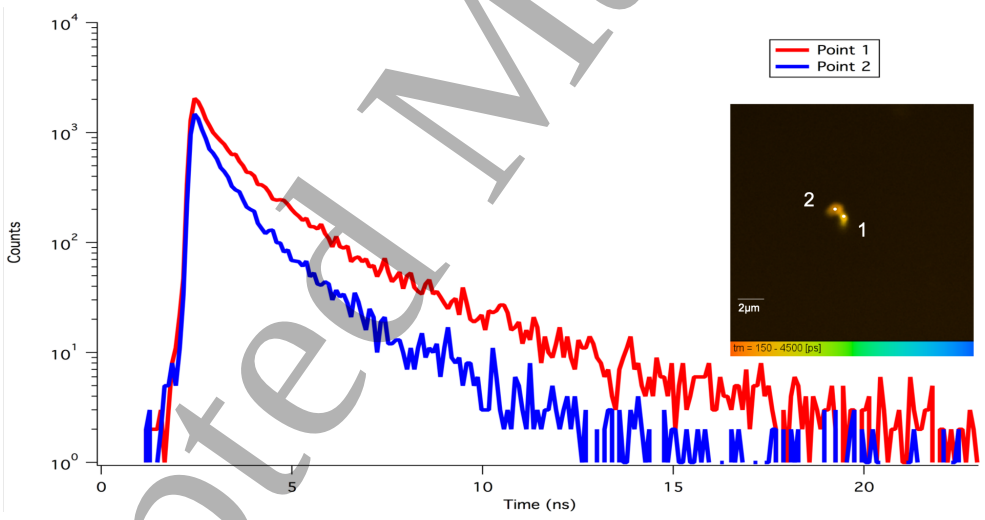

Figure 6: Representative fluorescence decay profiles of $P3^+$ in DMSO from two positions in the aggregate.

The time dependence of the formation of the τ_3 component for each polymer is plotted in Figure 7(a). Both lobes of the $P3^+$ aggregate reach their maximum value of τ_3 in approximately half the time required for the $P1^+$ and $P2^+$ samples. Intensity profiles across the aggregated regions were calculated using ImageJ as a function of irradiation time for each polymer. The size of the photo-induced aggregates and the time taken to reach these sizes are summarised in Figure 7(b). Polymers $P1^+$ and $P2^+$ grow to nearly identical sizes and at similar rates, however, $P3^+$ shows grows fast initially, but the overall size of the aggregates reaches its maximum at a slightly longer irradiation time.

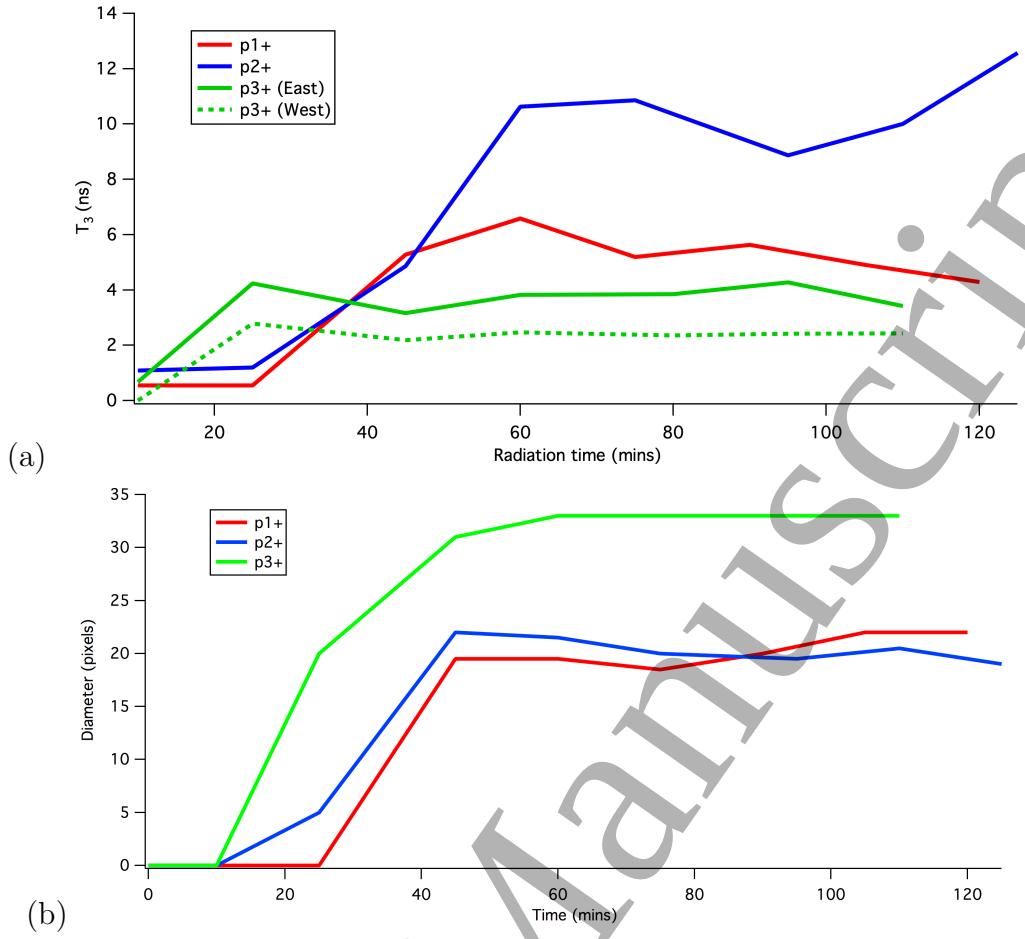

Figure 7: (a) τ_3 component and (b) Diameter of photo-aggregated region as a function of irradiation time.

It is worth reiterating that the $P3^+$ exhibits different photophysical behaviour to the other two polymers. The absorption maxima of $P1^+$ and $P2^+$ are located at 358 and 346 nm, respectively, whereas the absorption maximum of $P3^+$ is significantly to the red (432 nm) of the other polymers. This was attributed to the strong intramolecular charge transfer (ICT) from the electron-donating TPE to the electron-withdrawing benzo-2,1,3-thiadiazole moiety.[11] It may be possible that this could be associated with the observed difference in aggregation behaviour between $P3^+$ and the other two polymers.

The mechanism of the photon pressure-induced aggregation is not known definitively. Dynamic light scattering measurements on the same solutions used for the photo-aggregation indicate that aggregates of 100-300 nm diameter exist in the solution of each CPE sample prior to the application of the IR beam, so at least in the present case, we speculate that the photoaggregation is initiated by optically trapping adequately sized small clusters, which then accumulate at the focal point. The continued aggregation of the CPE chromophores leads to restriction of the non-radiative deactivation (rotational freedom within the TPE group) giving rise to longer-lived emission. The polymers continue aggregating to a diameter of ~2-3 μm, at which point the emission begins to decay on slightly shorter timescales, presumably due to self quenching.

4. Conclusions

We have demonstrated the value of using time-resolved emission imaging methods coupled with photon pressure-induced microparticle formation from photoluminescent conjugated polyelectrolytes in solution. In particular we show that maps of the individual decay time components (e.g. τ_3 in this case) can identify information that is masked in the average lifetime maps. The CPEs studied exhibit increases in the timescales of their emission decay as they photo-aggregate, attributed to reduced non-radiative deactivation of the excited state as a consequence of restricted motion within the TPE group. The observed differences in the aggregation of the $P3^+$ compared to the other polymers appear to correlate with the different photophysical properties of the CPEs.

5. Acknowledgments

The authors acknowledge the support of the Australian Research Council Centre of Excellence in Exciton Science (CE170100026). We also thank Mr. Heyou Zhang for assistance with the DLS measurements. The authors have declared that no conflicting interests exist.

6. References.

[1] A. Ashkin, "Acceleration and trapping of particles by radiation pressure," Phys. Rev. Lett. **24**, 156–159 (1970).

[2] A. Ashkin, *Optical Trapping and Manipulation of Neutral Particles Using Lasers* (World Scientific, 2006).

[3] T. Sugiyama, K.-i. Yuyama, and H. Masuhara, "Laser Trapping Chemistry: From Polymer Assembly to Amino Acid Crystallization," Acc. Chem. Res. **45**, 1946–1954 (2012).

[4] V. L. Y. Loke, T. Asavei, S. Parkin, N. R. Heckenberg, H. Rubinsztein-Dunlop, and T. A. Nieminen, "Driving optical micromachines with orbital angular momentum," in *Twisted photons: Applications of light with orbital angular momentum*, J. P. Torres and L. Torner, eds. (Wiley-VCH Verlag, Weinheim, Germany, 2011), pp. 93–116.

[5] M. Ishikawa, H. Misawa, N. Kitamura, and H. Masuhara, "Poly(N-isopropylacrylamide) Microparticle Formation in Water by Infrared Laser-Induced Photo-Thermal Phase Transition," Chem. Letts. pp. 481–484 (2004).

[6] K. Crawford and K. Hughes, "Rapid Formation and Spectroscopic Observation of Polystyrene," J. Phys. Chem. B **101**, 864–870 (1997).

[7] I. Jacob, E. Edri, E. Lasnoy, S. Piperno, and H. Shpaisman, "Influencing colloidal formation with optical traps," Soft Matter **13**, 706–710 (2017).

[8] S. Ito, Y. Tanaka, H. Yoshikawa, Y. Ishibashi, H. Miyasaka, and H. Masuhara, "Confinement of Photopolymerization and Solidification with Radiation Pressure," J. Am. Chem. Soc. **133**, 14 472–14 475 (2011).

[9] P. Borowicz, J.-I. Hotta, K. Sasaki, and H. Masuhara, "Chemical and Optical Mechanism of Microparticle Formation of Poly(N-vinylcarbazole) in N, N-Dimethylformamide by Photon Pressure of a Focused Near-Infrared Laser Beam," J. Phys. Chem. B **102**, 1896–1901 (1998).

[10] T. A. Smith, J.-I. Hotta, K. Sasaki, H. Masuhara, and Y. Itoh, "Photon Pressure-Induced Association of Nanometer-Sized Polymer Chains in Solution," J. Phys. Chem. B **103**, 1660–1663 (1999).

[11] M. Gao, Y. Hong, B. Chen, Y. Wang, W. Zhou, W. W. H. Wong, J. Zhou, T. A. Smith, and Z. Zhao, "AIE conjugated polyelectrolytes based on tetraphenylethene for efficient fluorescence imaging and lifetime imaging of living cells," Polym. Chem. **8**, 3862–3866 (2017).

[12] J. Zhou, Y. Wang, Y. Hong, B. Chen, M. Gao, B. Zhang, T. A. Smith, W. W. H. Wong, and Z. Zhao, "A

water-soluble, AIE-active polyelectrolyte for conventional and fluorescence lifetime imaging of mouse neuroblastoma neuro-2A cells," Journal of Polymer Science, Part A: Polymer Chemistry **56**, 672–680 (2018).

[13] A. Sillen and Y. Engelborghs, "The Correct Use of 'Average' Fluorescence Parameters," Photochemistry and Photobiology **67**, 475–486 (1998).

[14] A. Usman, W.-Y. Chiang, and H. Masuhara, "Optical trapping and polarization-controlled scattering of dielectric spherical nanoparticles by femtosecond laser pulses," Journal of Photochemistry and Photobiology A: Chemistry **234**, 83–90 (2012).

[15] W.-Y. Chiang, A. Usman, T. Sugiyama, J. Hofkens, and H. Masuhara, "Femtosecond Laser Trapping Dynamics of Nanoparticles: A Single Transient Assembly Formation Leading to Their Directional Ejection," J. Phys. Chem. C **122**, 13 233–13 242 (2018).